Environmental Health Perspectives
Vol. 65, pp. 21-27, 1986

Primary Structure and Spectroscopic Studies of Neurospora Copper Metallothionein

by Mariano Beltramini* and Konrad Lerch†‡

When *Neurospora crassa* is grown in the presence of Cu(II) ions, it accumulates the metal with the concomitant synthesis of a low molecular weight copper-binding protein. The molecule binds 6 g-atom of copper per mole protein (M_r = 2200) and shows a striking sequence homology to the zinc- and cadmium-binding vertebrate metallothioneins. Absorption, circular dichroism, and electron paramagnetic resonance spectroscopy of Neurospora metallothionein indicate the copper to be bound to cysteinyl residues as a Cu(I)-thiolate complex of the polymeric μ-thiolate structure $[Cu(I)_6RS_7]^-$. This metal-binding mode is also in agreement with the unusual luminescence of the protein. Spectral perturbation studies with $HgCl_2$ and *p*-(chloromercuri)benzoate suggest that the 6 Cu(I) ions are coordinated to the seven cysteinyl residues in the form of a single metal cluster. Neurospora apometallothionein is also capable of binding *in vivo* group IIB metal ions [Zn(II), Cd(II), and Hg(II)] as well as paramagnetic Co(II) ions with an overall metal-to-protein stoichiometry of 3. The spectroscopic properties of the fully substituted forms are indicative of a distorted tetrahedral coordination. However, metal titration of the apoprotein shows the third metal ion to be differently coordinated than the other two metal ions. This difference can be explained by the presence of only seven cysteine residues in Neurospora metallothionein as opposed to nine cysteine residues in the three-metal cluster of the mammalian metallothioneins.

Introduction

Metallothioneins (MTs) are a class of low molecular weight, cysteine-rich proteins binding high amounts of metal ions such as Cd, Zn, and/or Cu. After the first isolation and characterization of a Zn- and Cd-containing MT from horse kidney (*1*), most of the attention was focused on the proteins isolated from mammalian species. However, further studies have shown the wide occurrence of these proteins among microorganisms, plants, and invertebrates (*2*). In contrast to MTs from higher eucaryotic organisms binding different metal ions, fungal MTs contain exclusively copper (*3*). In this paper, the primary structure and the spectroscopic properties of the Cu-MT isolated from the ascomycete *Neurospora crassa* are reviewed.

Primary Structure

When *Neurospora crassa* is grown on a Cu-supplemented medium, almost 10% of the metal taken up by the organism appears to be bound to a low molecular weight protein present in the cytosolic fraction of the cells (*4*). By a combination of gel filtration and DEAE-cellulose ionic exchange chromatography under anaerobic conditions, this copper-binding protein can be isolated to a high degree of purity.

As shown in Table 1, the protein has a rather rudimentary amino acid composition and is lacking aromatic amino acids and histidine. Furthermore, it is characterized by a very high content of cysteine, serine, and glycine. The native protein contains no free sulfhydryl groups or disulfides, which indicates that all seven cysteines are involved in metal binding. This conclusion is in agreement with the low pH (< pH 1.0) required to displace the metal from the protein.

These properties allow to classify this copper-binding protein among the family of metallothioneins. This conjecture is further supported by amino acid sequence analysis (*4*). As shown in Figure 1, the amino acid sequence of Neurospora Cu-MT is strikingly similar to those of the NH_2-terminal region of the Zn- and Cd-containing MTs from vertebrates. In particular, the seven cysteinyl residues of Neurospora Cu-MT are found in the same positions as the first seven cysteines of the NH_2-terminal part of vertebrate Zn- and Cd-containing MTs (*4*). Furthermore, the primary structure of Neurospora

*Department of Biology, University of Padova, Via Loredan 10, I-35131, Padova, Italy.
†Biochemisches Institut der Universität Zürich, Winterthurerstrasse 190, CH-8057 Zürich, Switzerland.
‡Author to whom correspondence and reprint requests should be addressed.

```
                        1       5           10          15          20          25
Human   MT-2  Ac-M D P N C S C A A G D S C T C A G S C K C K E C K C T S ...
Equine  MT-2  Ac-M D P N C S C V A G E S C T C A G S C K C K Q C R C A S ...
Mouse   MT-1  Ac-M D P N C S C S T G G S C T C T S S C A C K D C K C T S ...
Plaice        Ac-M D P - C E C S K T G T C N C G G(S)C T C K N C G C T ...
Neurospora          G D C G C S G A S S C N C G S G C S C S N C G S K
```

FIGURE 1. Sequence comparison of Neurospora Cu-MT (*4*) with that of the NH_2-terminal part of invertebrate and vertebrate species. The sequences are: human MT-2 (*19*), equine MT-1 (*20*), mouse MT-1 (*21*), plaice (*22*). One-letter symbols: A = alanine, C = cysteine, D = aspartic acid, E = glutamic acid, G = glycine, K = lysine, M = methionine, N = asparagine, P = proline, S = serine, T = threonine. Other symbols: Ac = acetyl. Identical residues are indicated by boxes.

Cu-MT shows the occurrence of three Cys—X—Cys sequences (residues 5,6,7–13,14,15–19,20,21), where X stands for a residue different from cysteine. This unique arrangement is a typical feature of all vertebrate MTs studied so far (*2*). It was proposed to be essential for metal complexation and indicates that the cysteine residues are specific metal ligands (*2*). Despite the fact that the amino acids apart from the cysteines are highly variable, the overall sequence homology between Neurospora Cu-MT and the NH_2-terminal part of mammalian forms is in the order of 32% (*5*).

The primary structure of Neurospora Cu-MT has been recently confirmed by gene sequence analysis (*6*) which, furthermore, unambiguously shows that this small MT is a distinct protein and not the product of a proteolytic cleavage of a larger molecule occurring upon isolation.

Spectroscopic Properties

The spectroscopic properties of Neurospora Cu-MT arise predominantly from the metal-to-protein complexation. This is borne out by a comparison of the absorption and the circular dichroism (CD) spectra of native protein with those of the apoform (*7*). In agreement with the lack of aromatic amino acids, the absorption spectrum of apoMT is negligible above ~ 260 nm (Fig. 2). The far-UV band at $\lambda < 200$ nm can be attributed to $\pi-\pi^*$ and $n-\pi^*$ amide transitions of the peptide moiety (*7,8*). The binding of Cu intensifies the far-UV absorption, introduces the characteristic shoulder at ~ 250 nm, and is responsible for the appearance of the red edge of the spectrum extending to 400 nm (Fig. 2).

In contrast to the poorly resolved absorption spectrum, the CD profile shows the presence of at least five Cotton bands in the region $230 \leq \lambda \leq 400$ nm, with maxima at 230 (+), 245 (−), 270 (+), 295 (−), and 355 (+) (Fig. 2). These features arise from asymmetry in the metal-protein complex because they are absent in the apoprotein (Fig. 2). Again, the negative band of apoMT can be attributed to amide transitions.

The spectroscopic properties of Neurospora Cu-MT are indicative of copper binding in the form of an asymmetric Cu(I)-thiolate complex $[Cu(I)_6RS^-_7]^-$. Accordingly, the protein is EPR-silent and lacks absorption in the visible region diagnostic for $d-d$ transitions of Cu(II) complexes (*9*). Although the Gaussian analysis is rather difficult in the case of the broad and featureless absorption profile of Neurospora Cu-MT, the red edge of the spectrum would arise from the lowest-energy charge-transfer transition, in agreement with the presence of two bands in the CD spectrum at $\lambda > 280$ nm.

Upon excitation in the ultraviolet, Neurospora Cu-MT emits an unusual orange-yellow luminescence (*7*). The

Table 1. Amino acid composition of Neurospora Cu-MT.

Residue		Content, %	Number of residues: Amino acid analysis	Number of residues: Sequence
Asx			3.0	
Asp		4		1
Asn		8		2
Ser		28	6.9	7
Gly		24	5.9	6
Ala		4	1.1	1
Cys		28	7.0	7
Lys		4	1.0	1
Total residues		100	24.9	25
Molecular weight	2220			
Metal content	13	6 g-atoms/mole		
Molecular weight including Cu	2600			

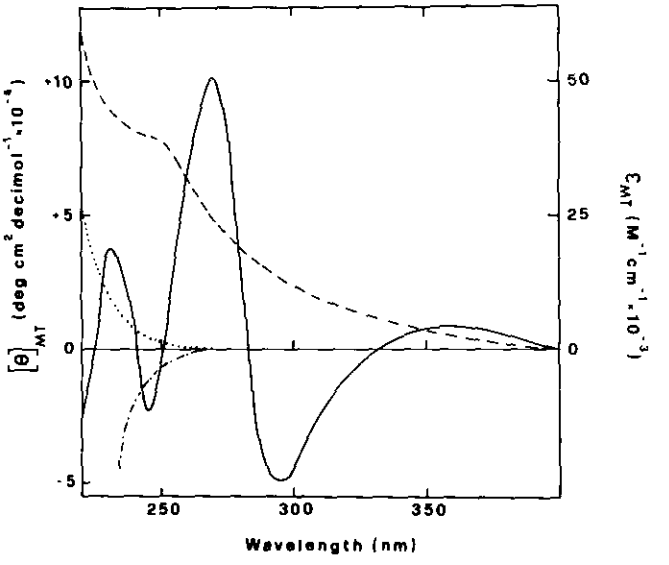

FIGURE 2. Absorption (--) and circular dichroism (——) spectra of Neurospora Cu-MT. The absorption (··) and the circular dichroism (–·–) spectra of apoMT (pH < 1) are also shown (*23*). ϵ and $[\theta]$ are calculated on a per-mole MT basis.

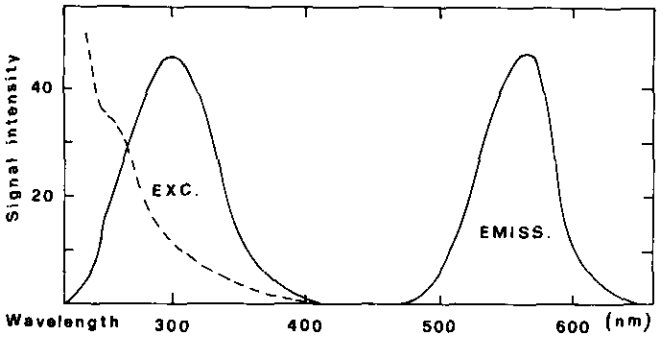

FIGURE 3. Observed excitation (exc.) and emission (emiss.) spectra of Neurospora Cu-MT (——); corrected excitation spectrum (--) (*23*).

emission spectrum recorded at 283°K consists of a broad band with a maximum at 565 nm and an unusually large Stokes shift (Fig. 3). No fine structure is evident at 77°K, and at this temperature the lifetime τ_0 for the excited state deactivation is in the order of 160 μsec. The quantum yield of Neurospora Cu-MT is 0.013 at 283°K (Table 2). However, a twofold increase is observed in D_2O, and a threefold increase results both from the absence of O_2 and in more viscous media (50% glycerol-water). The corrected excitation spectrum (Fig. 3) shows the same profile as the absorption spectrum, thus indicating that the luminescence emission is an inherent property of the Cu(I)–thiolate complex. This conclusion is confirmed by the disappearance of the luminescence observed upon metal displacement by HCl (pH < 1.0) and by the lack of emission of the oxidized protein where both the metal and the sulfur ligands are oxidized (*9,10*).

As pointed out earlier (*11*), metal complexes involving metal ions which are diamagnetic, easily oxidized, and displaying charge-transfer transitions are expected to be luminescent. As Neurospora Cu-MT fulfills all these criteria, the luminescence could be attributed to transitions of the charge-transfer type of the Cu(I)–thiolate complex.

Luminescence emission similar to that of Neurospora Cu-MT is observed also in the case of low molecular weight Cu(I) complexes containing ligands such as cysteine, reduced glutathione, and 2-mercaptoethanesulfonic acid (Table 2). However, there exists a strong difference between Neurospora Cu-MT and the model compounds, in that only the protein emits in aqueous solutions at room temperature. The luminescence of the low molecular weight complexes is observed either in the dried state or at liquid nitrogen temperature. As the low molecular weight compounds strongly interact with the solvent, their luminescence emission is expected to be highly quenched by solvent vibrations. Hence, the considerable luminescence emitted by the protein could be explained on the basis of a partial shielding of the luminescence copper–thiolate luminophore elicited by the protein backbone. This interpretation is in agreement with the above-mentioned effects of the solvent on the emission quantum yield (*7*). Although the peptide backbone is rather short and simple, lacking any bulky hydrophobic amino acid residues, a compact tertiary structure can be induced by the presence of several metal–thiolate bonds which could be responsible also for the considerable stability of the protein against heat denaturation and the effects of chaotropic agents (*12*).

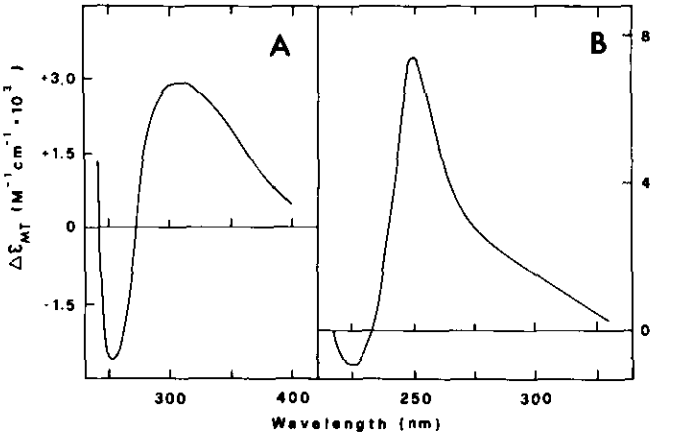

FIGURE 4. Difference absorption spectra of Neurospora Cu-MT observed in the presence of (*A*) $HgCl_2$ and (*B*) *p*-(chloromercury) benzoate (PCMP) present in a twofold excess over the metallothionein concentration (*23*).

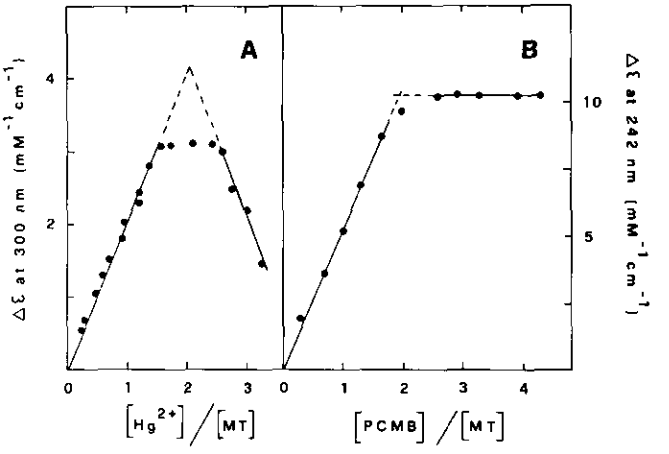

FIGURE 5. Absorption titration of Neurospora Cu-MT with (*A*) $HgCl_2$ and (*B*) PCMB (*7*). Hg^{2+}/MT, PCMB/MT represent the mercury-to-protein ratios.

Spectroscopic Perturbation Studies

The spectroscopic properties of Neurospora Cu-MT are distinctly modified by addition of Hg(II) ions or *p*-(chloromercury)benzoate (PCMB). The binding of both species has been studied by difference spectrophotometry and titration experiments (*7*).

The difference spectra of either Hg(II) or PCMB-treated Cu-MT against native Cu-MT show signals whose intensity and shape changes according to the Hg-to-protein stoichiometry (Hg(II)-MT) (Fig. 4*A*). Thus, at 0 < Hg(II)-MT ≤ 2, the difference spectrum shows a ~ 300 nm (+) and a ~ 255 nm (−) band. Both bands

Table 2. Emissive properties of Neurospora Cu-MT and different Cu(I)-mercaptide complexes.[a]

Sample	Condition	λ_{emiss}, nm	Quantum yield Q	Half-band width $\Delta\lambda$, nm
Neurospora Cu-MT	H_2O[b]	565	0.013	62[c]
	D_2O[b]	565	0.026	62
	Argon, H_2O[b]	565	0.033	62
	Glycerol, 50%	565	0.033	62
Cu(I)-cysteine	Dried sample	585	—	54[d]
Cu(I)-glutathione	Dried sample	575	—	51[d]
Cu(I)-2-mercaptoethanesulfonate	Glycerol, 50%, 77°K	520	—	86

[a] Data of Lerch and Beltramini (*23*) unless otherwise noted.
[b] Measured in 20 mM potassium phosphate, pH 7.5, 283°K.
[c] Data from Beltramini and Lerch (*7*).
[d] Data from Anglin et al. (*24*).

increase in intensity, relatively to their positive or negative value (Fig. 4*A*). At Hg(II)/MT > 2, the spectral changes are more complicated, and a decrease in the 300 nm difference band is observed. Similar results are seen with PCMB (Fig. 4*B*), where two bands at 250 nm (+) and 225 nm (−) are visible. The results of spectrophotometric titrations show the presence of distinct breaking points at both Hg(II)-MT = 2 and PCMB-MT = 2 (Fig. 5). The difference bands at ~ 300 nm and 250 nm are typical of either Hg(II) or PCMB complexes involving thiol groups, thus indicating a direct complexation of the two mercurials to the cysteinyl residues of the protein. It should be pointed out that the binding of two Hg groups occurs without copper displacement as shown by gel filtration experiments (*7*). As expected, binding of Hg brings about also considerable changes in the chiroptical properties of native Cu-MT (Fig. 6). In addition, the luminescence emission is completely quenched. With respect to the latter effect, Hg(II) ions differ from PCMB in that they can quench the luminescence at a HG(II)-to-protein ratio of 1; the effect is linearly correlated with the amount of Hg(II) bound and is independent from the concentration of the protein (Fig. 7*A*). In contrast, the quenching brought about by PCMB is a nonlinear function of the PCMB-to-MT ratio; it depends on the MT concen-

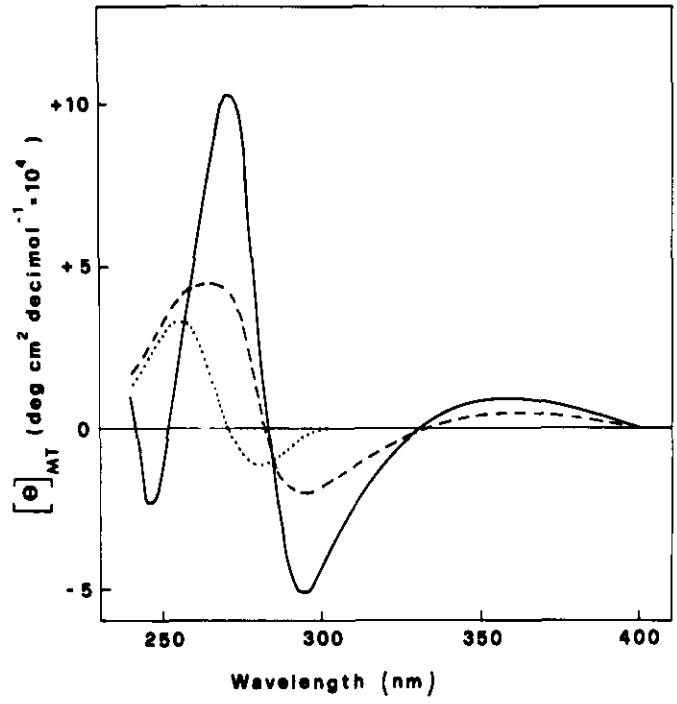

FIGURE 6. Circular dichroism spectra of Neurospora Cu-MT in the absence (——) and in the presence of 1.0 Hg/MT (--) and 2.0 Hg/MT (· · ·) (*7*).

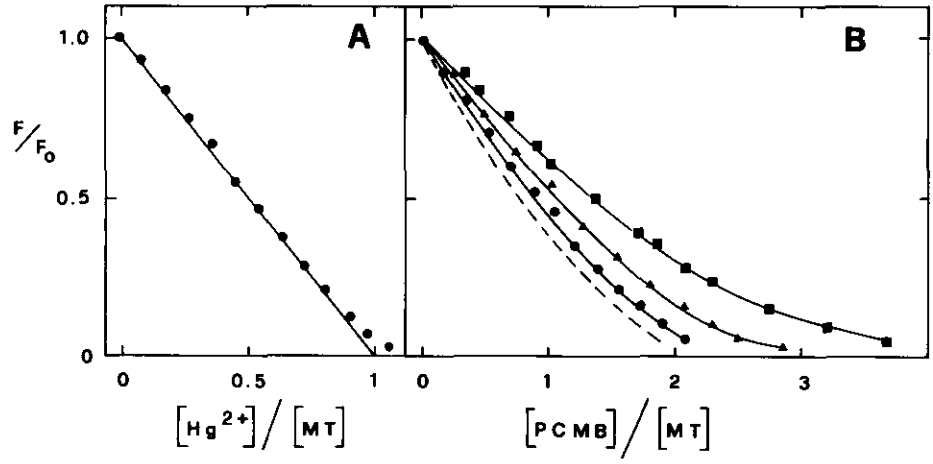

FIGURE 7. Luminescence quenching of Neurospora Cu-MT with (*A*) $HgCl_2$ and (*B*) PCMB. (*A*) Plot expected in the case of the proportionality between Hg^{2+}/MT and the quenching effect; (●) experimental points. In (*B*) the symbols are relative to MT concentrations of (■) 8.0 μM, (▲) 19.33 μM, and (●) 38.67 μM; (--) calculated plot when the protein concentration is extrapolated to infinity. F_0, and F denote emission intensity in the absence or in the presence of quencher, respectively, measured at the emission maximum (λ = 565 nm) (*7*).

Table 3. Comparisons of the absorption and chiroptical maxima of Zn(II)-, Cd(II)- and Hg(II)-substituted MTs with the calculated values based on optical electronegativities for T_d symmetry complexes.[a]

Metal derivative	Zn(II)-MT	Cd(II)-MT	Hg(II)-MT
Position of the metal-induced shoulder in the difference spectrum			
λ (nm); ν (μm^{-1})	205; 4.88	225; 4.44	283; 3.53
$\Delta\epsilon \times 10^{-3}$ ($M^{-1}cm^{-1}$)[b]	16.1	17.0	8.8
Position of the first Cotton band			
λ (nm); ν (μm^{-1})	232; 4.31	243; 4.11	280; 3.57
$[\Theta] \times 10^{-3}$ (degr. cm^2 $decmol^{-1}$)[a]	5.0	8.4	2.1
Calculated position of the LMCT band			
λ (nm); ν (μm^{-1})	232; 4.31	249; 4.02	312; 3.21
Position of the metal-induced shoulder in mammalian MT[c]			
λ (nm); ν (μm^{-1})	220; 4.55	245; 4.08	308; 3.30

[a] Data of Beltramini et al. (*8*) unless otherwise noted.
[b] Δε and [Θ] are calculated on a per mole MT basis.
[c] Data from Vašák et al. (*16*).

tration and is complete at a PCMB-to-MT ratio of 2 (Fig. 7*B*). This stoichiometry is also confirmed by the quenching curve analysis which is in agreement with a random binding model involving the presence of two nonequivalent PCMB binding sites characterized by a rather low affinity ($K_d \sim 5 \times 10^{-6}$ M) (*7,13*). Taken together, these results suggest that the 6 Cu(I) ions bound behave as a metal cluster similar to the mammalian MTs (*5*). However, the marked difference in the sulfur-to-metal ratio between Neurospora Cu-MT (1.1 : 1) and mammalian MTs (3 : 1) strongly argues for a different geometry of the complex.

In Figure 8 is shown a schematic model for the Cu(I)-thiolate complex of Neurospora Cu-MT. In this model the six Cu(I) ions are complexed to five cysteinyl residues bridging two Cu(I) ions each and to two terminal residues coordinating a single Cu(I) ion. These two monocoordinated sulfur ligands provide two additional binding sites for mercurials.

Metal Substitution Studies

Neurospora MT differs from mammalian proteins in that it binds *in vivo* cuprous ions exclusively. Furthermore, in contrast to mammalian proteins which are synthesized upon exposure to different metal ions (*2*), the induction of Neurospora Cu-MT is strictly dependent on Cu. Given the striking sequence homology to the NH_2-terminal part of mammalian MTs, it was of interest to study *in vitro* the binding of group II-B metal ions to Neurospora apoMT. Similarly to the three-metal cluster formed by the NH_2-region of mammalian MTs (*14,15*), Neurospora apoMT binds 3 g-atoms per mole protein of either group II-B metal ions (Zn, Cd, Hg) or paramagnetic Co(II) ions. This derivative behaves as a monomer, eluting on Sephadex G-50 at an apparent molecular weight of 2700 D (*8*). The electronic absorption and circular dichroism properties of the derivative are remarkably similar to those reported for the mammalian proteins (Table 3): the lowest-energy metal-induced spectroscopic features are red-shifted in the order Zn < Cd < Hg. As documented for mammalian proteins (*16*), this red shift can be explained on the basis of Jørgensen's concept of optical electronegativity of ions involved in a complex having a T_d microsymmetry (*17*). Although the protein is capable of binding three metal ions per protein molecule, the complexes involving two or three metal ions are spectroscopically different. This is seen by spectrophotometric titrations with both Cd(II) and Hg(II) showing a breaking point at a metal-to-protein ratio of 2 (Fig. 9).

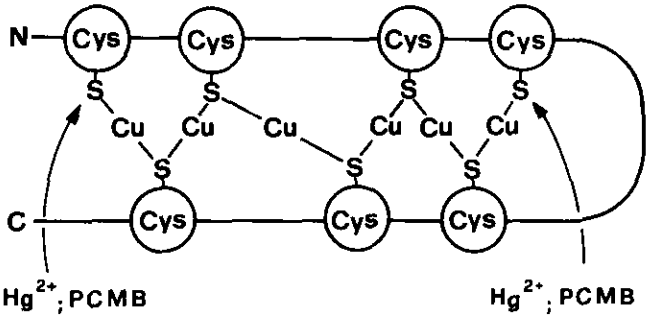

FIGURE 8. Schematic model for the metal-sulfur complex in Neurospora Cu-MT. The arrows indicate the hypothetical binding sites for mercurials (*4*).

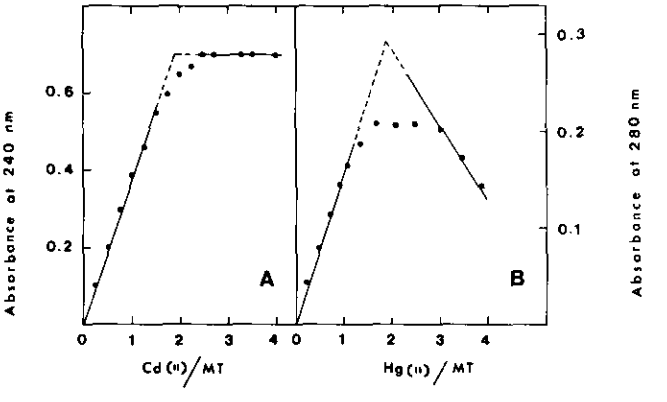

FIGURE 9. Spectrophotometric titration of Neurospora apoMT with either (*A*) Cd(II) or (*B*) Hg(II) ion. Cd(II)/MT and Hg(II)/MT indicate the Cd(II) or Hg(II) to MT ratios (*8*).

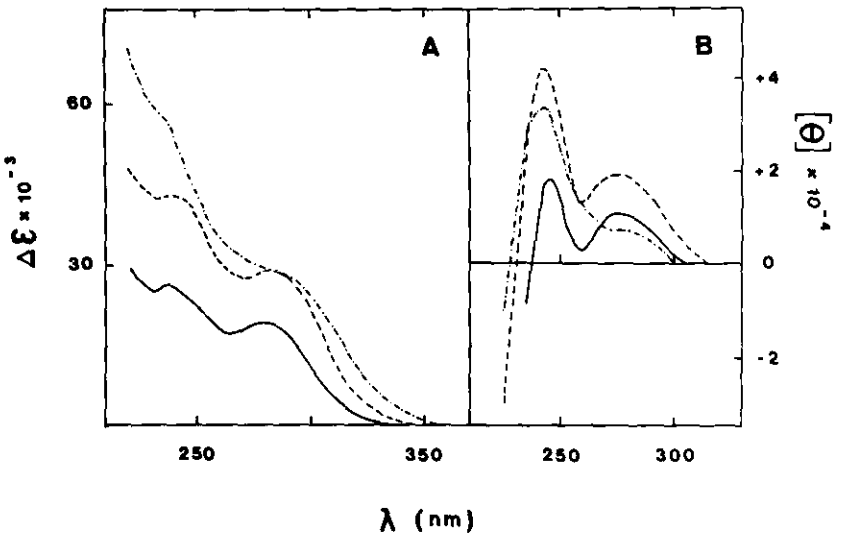

FIGURE 10. Difference electronic absorption (*A*) and CD spectra (*B*) of Hg(II)-substituted Neurospora apoMT. The spectra refer to the derivatives containing either (——) 1 mole, (--) 2 moles, or (–·–) 3 moles Hg(II) per mole of MT. The difference spectrum is recorded against an equimolar solution of apoMT in 0.05 M HCl as reference. Δε and [θ] are calculated on a per-mole MT basis (*8*).

Furthermore, in Figure 10 are reported both the electronic absorption and the CD spectra for the Hg(II) derivative containing 1, 2, and 3 Hg(II) equivalents per protein. The main contribution of the third metal ion bound occurs below 280 nm with no significant increase at 283 nm (Fig. 10*A*). Moreover, the CD spectra (Fig. 10*B*) of the Hg(II) derivatives show that the binding of the third Hg(II) ion brings about a decrease in the overall chiroptical features of the complex. This change most likely reflects the formation of a new Hg(II)–S-Cys complex (*8*). Similar results are obtained in the case of Co(II)-substituted MT. The absorption features are typical for a distorted tetrahedral Co(II)-thiolate coordination (*8,18*). The intensity of the *d-d* pattern arising from the spin-allowed $\nu_3[^4A_4(F)\text{-}^4T_1(P)]$ transition ($\lambda_{max} \sim 685$ nm) as well as that of the $S^- \rightarrow$ Co(II) charge transfer transition ($\lambda \sim 300$ nm) increases on going from 1 to 2 Co(II) per MT molecule while the coordination of the third metal ion results in a small spectral contribution (Fig. 11). Independent evidence for a distorted tetrahedral geometry is given by the electron paramagnetic resonance (EPR) spectra of the Co(II) derivative closely resembling that of a rhombically distorted high-spin Co(II) complex (*8*) (Fig. 12, left). Although the shape of the EPR signal is qualitatively the same at the different Co(II)-to-MT ratios, the signal intensity of the 2Co(II)-derivative is less than 30% of that measured for the species containing 1 Co(II) per MT, indicating antiferromagnetic spin-coupling between the two metal ions via a bridging sulfur (Fig. 12, right). A different coordination mode and/or the involvement of ligand(s) other than sulfur in the binding of the third metal ion may be

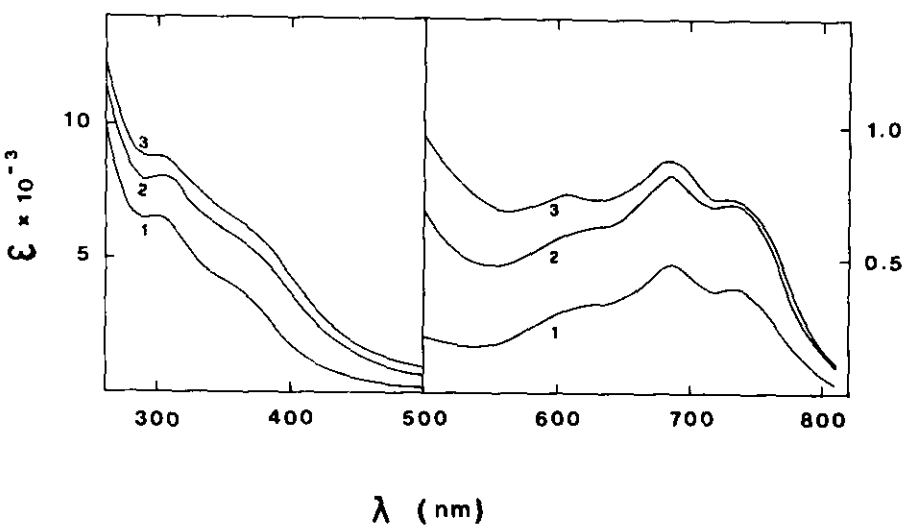

FIGURE 11. Electronic absorption spectrum of Co(II)-substituted Neurospora apoMT in 0.05 M Tris/HCl, pH 8.0. The numbers refer to the spectra obtained for the derivatives containing 1, 2, or 3 Co(II) per MT molecule. ε is calculated on a per-mole MT basis (*8*).

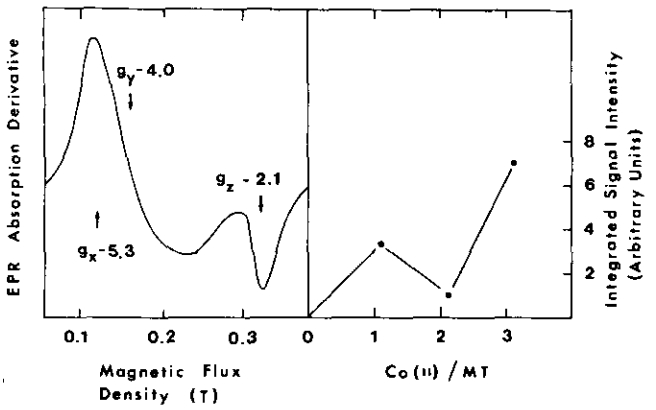

FIGURE 12. (Left) EPR spectrum of Co(II)-substituted Neurospora MT containing 3 Co(II) per MT molecule. Conditions: 0.53 mM Co(II)-MT in 0.05 M Tris/HCl, pH 8.0; microwave power 0.2 mW, microwave frequency 8.98 GH$_{\parallel}$; temperature 4°K. (Right) Dependency of the EPR signal intensity on Co(II)-protein ratio. The intensity plotted is calculated by double integration of the observed signal. Co(II)-MT indicates the Co(II)-to-MT molar ratios (*8*).

responsible for the increase in the EPR signal of the 3Co(II)-derivative (Fig. 12, right).

In conclusion, Neurospora apoMT is capable of binding three group-IIB metal ions in a tetrahedrally coordinated metal–sulfur complex. In this respect, it resembles closely the three-metal cluster of mammalian MTs whose amino acid sequence is remarkably similar to that of Neurospora MT. The difference in the coordination of the third metal ions most likely is a consequence of the presence of a smaller number of thiol ligands in Neurospora apoMT (seven cysteines) as opposed to the three-metal cluster of mammalian proteins (nine cysteines) (*15*).

This work was supported by Swiss National Science Foundation Grant No. 3.285-0.82 and the Kanton Zürich. We thank Genia de Vallier for typing this manuscript.

REFERENCES

1. Kägi, J. H. R., and Vallee, B. L. Metallothionein: a cadmium- and zinc-containing protein from equine renal cortex. J. Biol. Chem. 235: 3460–3465 (1960).
2. Kägi, J. H. R., and Nordberg, M. Metallothionein. Birkhäuser Verlag, Basel, 1979.
3. Lerch, K. The chemistry and biology of copper metallothioneins. In: Metal Ions in Biological Systems, Vol. 13 (H. Sigel, Ed.), M. Dekker, New York, 1981, pp. 299–318.
4. Lerch, K. Copper metallothionein, a copper-binding protein from *Neurospora crassa*. Nature 284: 368–370 (1980).
5. Kägi, J. H. R., Vašák, M., Lerch, K., Gilg, D. E. O., Hunziker, P., Bernhard, W. R., and Good, M. Structure of mammalian metallothionein. Environ. Health Perspect. 54: 93–103 (1984).
6. Münger, K., Germann, U. A., and Lerch, K. Isolation and structural organization of the *Neurospora crassa* copper metallothionein gene. EMBO J. 4: 2665–2668 (1985).
7. Beltramini, M., and Lerch, K. Spectroscopic studies on *Neurospora* copper metallothionein. Biochemistry 22: 2043–2048 (1983).
8. Beltramini, M., Lerch, K., and Vašák, M. Metal substitution of *Neurospora* copper metallothionein. Biochemistry 23: 3422–3427 (1984).
9. Beltramini, M., and Lerch, K. Copper transfer between *Neurospora* copper metallothionein and type 3 copper apoproteins. FEBS Letters 142: 219–222 (1982).
10. Beltramini, M., and Lerch, K. Luminescence properties of *Neurospora* copper metallothionein. FEBS Letters 127: 201–203 (1981).
11. Lytle, F. E. Solution luminescence of metal complexes. Appl. Spectrosc. 24: 319–326 (1970).
12. Beltramini, M., and Lerch, K., unpublished results.
13. Lehrer, S. S. Fluorescence and absorption studies of the binding of copper and iron to transferrin. J. Biol. Chem. 244: 3613–3617 (1969).
14. Otvos, J. D., and Armitage, I. M. Structure of the metal clusters in rabbit liver metallothionein. Proc. Natl. Acad. Sci. (U.S.) 77: 7094–7098 (1980).
15. Winge, D. R., and Miklossy, K. A. Domain nature of metallothionein. J. Biol. Chem. 257: 3471–3476 (1982).
16. Vašák, M., Kägi, J. H. R., and Hill, H. A. O. Zinc(II), cadmium(II), and mercury(II) thiolate transitions in metallothionein. Biochemistry 20: 2852–2856 (1981).
17. Jørgensen, C. K. Electron transfer spectra. Progr. Inorg. Chem. 12: 101–157 (1970).
18. Vašák, M., and Kägi, J. H. R. Metal thiolate clusters in cobalt(II)–metallothionein. Proc. Natl. Acad. Sci. (U.S.) 78: 6709–6713 (1981).
19. Kissling, M. M., and Kägi, J. H. R. Primary structure of human hepatic metallothionein. FEBS Letters 82: 247–250 (1977).
20. Kojima, Y., Berger, C., and Kägi, J. H. R. The amino acid sequence of equine metallothioneins. In: Metallothionein (J. H. R. Kägi and M. Nordberg, Eds.), Birkhäuser Verlag, Basel, 1979, pp. 153–161.
21. Huang, I.-Y., Yoshida, A., Tsunoo, H., and Nakajima, H. Mouse liver metallothioneins. Complete amino acid sequence of metallothionein-I. J. Biol. Chem. 252: 8217–8221 (1977).
22. Overnell, J., Berger, C., and Wilson, K. J. Partial amino acid sequence of metallothionein from the plaice (*Pleuronectes platessa*). Biochem. Soc. Trans. 9: 217–218 (1981).
23. Lerch, K., and Beltramini, M. *Neurospora* copper metallothionein: molecular structure and biological significance. Chem. Scripta 21: 109–115 (1983).
24. Anglin, J. H., Batten, W. H., Raz, E. A., and Sayre, R. M. Fluorescence of Cu, Au and Ag mercaptides. Photochem. Photobiol. 13: 279–281 (1971).